

Learning from Longitudinal Face Demonstration - Where Tractable Deep Modeling Meets Inverse Reinforcement Learning

Chi Nhan Duong, Kha Gia Quach, Khoa Luu , T. Hoang Ngan Le and Marios Savvides
CyLab Biometrics Center and the Department of Electrical and Computer Engineering,
Carnegie Mellon University, Pittsburgh, PA, USA

{chinhand, kquach, kluu, thihoanl}@andrew.cmu.edu, msavvid@ri.cmu.edu

Abstract

This paper presents a novel Generative Probabilistic Modeling under an Inverse Reinforcement Learning approach, named Subject-dependent Deep Aging Path (SDAP), to model the facial structures and the longitudinal face aging process of given subjects. The proposed SDAP is optimized using tractable log-likelihood objective functions with Convolutional Neural Networks based deep feature extraction. In addition, instead of using a fixed aging development path for all input faces and subjects, SDAP is able to provide the most appropriate aging development path for each subject that optimizes the reward aging formulation. Unlike previous methods that can take only one image as the input, SDAP allows multiple images as inputs, i.e. all information of a subject at either the same or different ages, to produce the optimal aging path for the subject. Finally, SDAP allows efficiently synthesizing in-the-wild aging faces without a complicated pre-processing step. The proposed method is experimented in both tasks of face aging synthesis and cross-age face verification. The experimental results consistently show the state-of-the-art performance using SDAP on numerous face aging databases, i.e. FG-NET, MORPH, AginG Faces in the Wild (AGFW), and Cross-Age Celebrity Dataset (CACD). The method also performs on the large-scale Megaface challenge 1 to demonstrate the advantages of the proposed solution.

1. Introduction

The problem of face aging targets on the capabilities to aesthetically *synthesize* the faces of a subject at the older ages, i.e. *age progression*, or the younger ages, i.e. *age regression* or *deaging*. This problem is applicable in various real-world applications from age invariant face verification, finding missing children to cosmetic studies. Indeed, the face aging has raised considerable attentions in computer vision and machine learning communities recently. Several

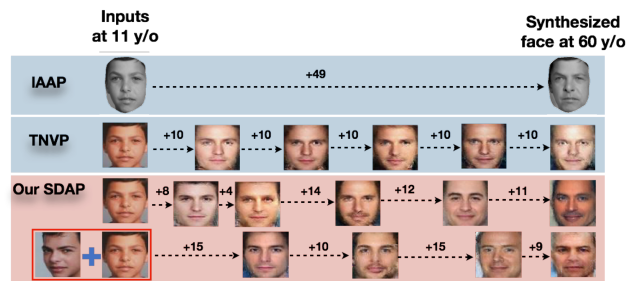


Figure 1: An illustration of age progression using direct (IAAP), step-by-step (TNVP) and our SDAP approaches. Instead of using a fixed aging development path for all inputs as in IAAP (the 1st row) and TNVP (the 2nd row), given a face and the target age, SDAP can discover the optimal aging development path (the 3rd row) for the subject. SDAP can also collect aging cues from multiple inputs to produce more aesthetical synthesis results (the 4th row).

breakthroughs along with numerous face aging approaches varying from anthropology theories to deep learning structures have been presented in literature. However, the synthesized face aging results in these previous approaches are still far to be perfect due to various challenging factors, such as heredity, living styles, etc. In addition, the face aging databases used in most methods to learn the aging processes are usually limited in both number of images per subject and the covered age ranges of each subject.

Both conventional and deep learning methods usually include two directions, i.e. *direct* and *step-by-step aging synthesis*, in exploring the temporal face aging features from training databases. In the former direction, these methods *directly* synthesize a face to the target age using the relationships between training images and their corresponding age labels. For example, the prototyping approaches [3, 9, 18] use the age labels to organize images into age groups and compute average faces for their prototypes.

Table 1: The comparison of the properties between our SDAP approach and other age progression methods. Deep learning (DL), Inverse Reinforcement Learning (IRL), Dictionary (DICT), Prototype (PROTO), Probabilistic Graphical Models (PGM), Log-likelihood (LL), Adversarial (ADV). Note that \times indicates *unknown* or *not directly applicable* properties.

	Our SDAP	TNVP [14]	CAAE[26]	RNN[24]	TRBM[15]	HFA[25]	IAAP[9]
Subject-dependent Aging Path	✓	×	×	×	×	×	×
Multiple Input Optimization	✓	×	×	×	×	×	×
Tractable	✓	✓	✓	✓	×	✓	×
Non-Linearity	✓	✓	✓	✓	✓	×	×
Model Type	DL + IRL	DL	DL	DL	DL	DICT	PROTO
Architecture	PGM+CNN	PGM+CNN	CNN	CNN	PGM	Bases	×
Loss Function	LL	LL	ADV+ ℓ_2	ℓ_2	LL	LL+ ℓ_0	×

Then, the difference between source-age and target-age prototypes is applied directly to the input image to obtain the age-progressed face at the target age. Similarly, the Generative Adversarial Networks (GAN) approach [26] models the relationship between high-level representation of input faces and age labels by constructing a deep-neural-network generator. This generator is then incorporated with the target age labels to synthesize the outputs. Although these kinds of models are easy to train, they are *limited* in capabilities to synthesize faces *much older* than the input faces of the same subject, e.g. directly from ten to 60 years old. Indeed, the progression of a face at ten years old to the one at 60 years old in these methods usually ends up with a synthesized face using 10-year-old feature plus wrinkles.

Meanwhile, the latter approaches [14, 15, 19, 24, 25] *decomposes* the long-term aging process into *short-term* developments and focuses on the aging transform embedding between faces of two *consecutive* development stages. Using these learned transformation, these methods step-by-step generate progressed faces from one age group to the next until reaching the target ones. These modeling structures can efficiently learn the temporal information and provide more age variation even when a target age is very far from the input age of a subject. However, the main *limitation* of these methods is the *lack* of longitudinal face aging databases. The longest training sequence usually contains only three or four images per subject.

However, both directions suffer from the same problems. Even though a subject in training/testing set has multiple images at the same age, there is *only one* image used to learn/synthesize in these methods. The other images are usually wastefully *ignored*. In addition, the aging transformation embedding in these approaches is only able to proceed on images from *two* age groups. Finally, both directions apply *the same* aging development path for all subjects which is not true in reality. Instead, each subject should have his/her own aging development.

Contributions of this work: This paper presents a novel Generative Probabilistic Modeling (GPM) under an Inverse

Reinforcement Learning (IRL) approach, named *Subject-dependent Deep Aging Path (SDAP)*, to face age progression. In this approach, the aging transformation embedding is designed using (1) a *tractable log-likelihood* density estimation with (2) Convolution Neural Network (CNN) structures and (3) a present of an *age controller* to indicate the amount of aging changes for synthesis. In this proposed structure, not only can a *smoother synthesis* across faces be produced but also the *usability* of aging data, i.e. all images of a subject in different or the same ages, is also improved for better transformation.

Far apart from previous methods, our proposed GPM approach enhances the capability to discover *the optimal* aging development path for *each* individual. This goal can be done by embedding the transformation over the whole aging sequence of a subject under an IRL framework.

In addition, instead of using pre-defined or add-hoc aging reward and objective functions as in most previous work, our proposed approach allows the algorithm to automatically come up with the *optimal objective formulation and parameters* via a data driven strategy in training. To the best of our knowledge, this work is the first one to design an IRL framework to model the longitudinal face aging. In our framework, the long-term age developments of individuals are represented as demonstrated aging sequences. Then, the SDAP model is constructed to capture the temporal face aging feature transformed in the whole sequence. During the model construction steps, an Aging Category-based Stochastic Policy Network is also learned to compute planning aging paths that are best fitted to the specific development of each subject.

2. Related work

This section reviews recent methods in face age progression. These methods can be technically classified into four categories, i.e. modeling, reconstruction, prototyping, and deep learning-based methods.

Modeling-based aging is one of the earliest categories presented face age progression. These methods usually

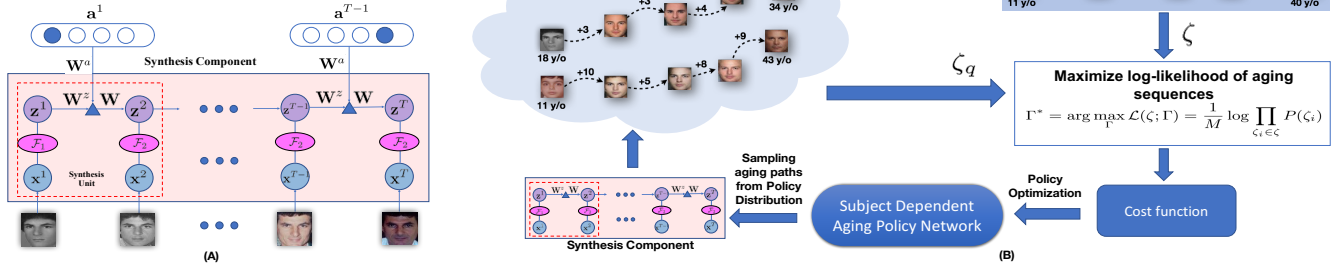


Figure 2: The structures of (A) a Synthesis Component as a composition of Synthesis Units, and (B) the Subject-Dependent Aging Policy Learning Framework.

model both facial shapes and textures using a set of parameters, and learn the face aging process via aging functions. Pattersons et al. [16] and Lanitis et al. [10] employed a set of Active Appearance Models (AAMs) parameters with four aging functions to model both the general and the specific aging processes. Luu et al. [13] combined familial facial cues to the process of face age progression. Geng et al. [7] presented the AGing pattErn Subspace (AGES) method to construct a subspace for aging patterns as a chronological sequence of face images. Tsai et al. [23] then enhanced the AGES using guidance faces corresponding to the subject’s characteristics to produce more stable results. Texture synthesis was also combined in the later stage to produce better facial details. Suo et al. [21, 20] introduced the three-layer And-Or Graph (AOG) of smaller parts, i.e. eyes, nose, mouth, etc., to model a face. Then, the face aging process was learned for each part using a Markov chain.

Reconstruction-based aging methods model aging faces by unifying the aging basis in each group. Yang et al. [25] represented person-specific and age-specific factors independently using sparse representation hidden factor analysis (HFA). Shu et al. [19] presented the aging coupled dictionaries (CDL) to model personalized aging patterns by preserving personalized facial features.

Prototyping-based aging methods employ the age prototypes to produce new face images. The average faces of all age groups are used as the prototypes [18]. Then, input face image can be progressed to the target age by incorporating the differences between the prototypes of two age groups [3]. Kemelmacher-Shlizerman et al. [9] presented to construct high quality average prototypes from a large-scale set of images. The subspace alignment and illumination normalization were also included in this system.

Deep learning-based aging approaches have recently achieved considerable results in face age progression using the power of deep learning. Duong et al. [15] intro-

duced Temporal Restricted Boltzmann Machines (TRBM) to represent the non-linear aging process with geometry constraints and spatial RBMs to model a sequence of reference faces and wrinkles of adult faces. Wang et al. [24] approximated aging sequences using a Recurrent Neural Networks (RNN) with two-layer Gated Recurrent Unit (GRU). Recently, the structure of Conditional Adversarial Autoencoder (CAAE) is also applied to synthesize aged images in [2]. Duong et al. [14] proposed a novel generative probabilistic model, called Temporal Non-Volume Preserving (TNVP) transformation, to model a long-term facial aging process as a sequence of short-term stages.

3. Our Proposed Method

In this section, we first present our novel approach to model the facial structures and their relationships in Subsection 3.1. Then, our IRL learning approach to the longitudinal face aging modeling is detailed in Subsection 3.2.

3.1. Aging Embedding with Age Controller

The proposed architecture consists of three main components, i.e. (1) latent space mapping, (2) aging transformation, and (3) age controller. Our age controller provides the capability of defining how much age variation should be added during synthesis. Using this structure, our model is flexible to age different ways corresponding to the input faces. Moreover, it also helps to maximize the usability of training aging data.

Structures and Variable Relationship Modeling: Our graphical model (Fig. 2(A)) consists of three sets of variables: observed variables $\{x^{t-1}, x^t\} \in \mathcal{I}$ encoding the textures of face images in the image domain $\mathcal{I} \subset \mathbb{R}^D$ at two stages $t-1$ and t ; their corresponding latent variables $\{z^{t-1}, z^t\} \in \mathcal{Z}$ in the latent space \mathcal{Z} ; and an aging controller variable $a^{t-1} \in \mathcal{A} \subset \mathbb{R}^{N_a}$. The aging controller

\mathbf{a}^{t-1} is represented as a one-hot vector indicating how many years old the progression process should perform on \mathbf{x}^{t-1} . The bijection functions $\mathcal{F}_1, \mathcal{F}_2$, mapping from the observation space to the latent space, and the aging transformation \mathcal{G} are defined as in Eqn. (1).

$$\begin{aligned} \mathcal{F}_1, \mathcal{F}_2 : \mathcal{I} &\rightarrow \mathcal{Z} \\ \mathbf{x}^{t-1} &\mapsto \mathbf{z}^{t-1} \sim \mathcal{F}_1(\mathbf{x}^{t-1}; \boldsymbol{\theta}_1) \\ \mathbf{x}^t &\mapsto \bar{\mathbf{z}}^t \sim \mathcal{F}_2(\mathbf{x}^t; \boldsymbol{\theta}_2) \\ \mathcal{G} : \mathcal{Z}, \mathcal{A} &\rightarrow \mathcal{Z} \\ \mathbf{z}^{t-1}, \mathbf{a}^{t-1} &\mapsto \mathbf{g}^t \sim \mathcal{G}(\mathbf{z}^{t-1}, \mathbf{a}^{t-1}; \boldsymbol{\theta}_3) \end{aligned} \quad (1)$$

where $\boldsymbol{\theta} = \{\boldsymbol{\theta}_1, \boldsymbol{\theta}_2, \boldsymbol{\theta}_3\}$ denotes the set of parameters of $\mathcal{F}_1, \mathcal{F}_2, \mathcal{G}$, respectively. Then, the relationship between latent variables $\mathbf{z}^t, \mathbf{z}^{t-1}$ and \mathbf{a}^{t-1} is computed as $\mathbf{z}^t = \mathbf{g}^t + \bar{\mathbf{z}}^t$.

The interactions between latent variables $\{\mathbf{z}^{t-1}, \mathbf{z}^t\}$ and the aging controller variable \mathbf{a}^{t-1} are 3-way multiplicative. They can be mathematically encoded as in Eqn. (2).

$$g_i^t = \sum_{j,k} \hat{w}_{ijk} z_j^{t-1} a_k^{t-1} + b_i \quad (2)$$

where $\hat{\mathbf{W}} \in \mathbb{R}^{D \times D \times N_a}$ is a 3-way tensor weight matrix and \mathbf{b} is the bias of these connections. Eqn. (2) enables two important properties in the architecture. First, since \mathbf{a}^{t-1} is a one-hot vector, different controllers will enable different sets of weights to be used. Thus, it allows controlling the amount of aging information to be embedded to the aging process. Second, given the age controller, the model is able to use all images of a subject to enhance its performance.

In practice, the large number of parameters of the 3-way tensor matrix may have negative effects to the scalability of the model. Thus, $\hat{\mathbf{W}}$ can be further factorized into three matrices $\mathbf{W}^a \in \mathbb{R}^{f \times N_a}$, $\mathbf{W}^z \in \mathbb{R}^{f \times D}$, and $\mathbf{W} \in \mathbb{R}^{D \times f}$ with f factors by adopting [22] as in Eqn. (3).

$$\mathbf{g}^t = \mathbf{W}(\mathbf{W}^z \mathbf{z}^{t-1} \odot \mathbf{W}^a \mathbf{a}^{t-1}) + \mathbf{b} \quad (3)$$

where \odot stands for the Hadamard product.

The Log-likelihood: Given a face \mathbf{x}^{t-1} in the age group $t-1$, the probability density function can be formulated as,

$$\begin{aligned} p_{X^t}(\mathbf{x}^t | \mathbf{x}^{t-1}, \mathbf{a}^{t-1}; \boldsymbol{\theta}) &= p_{X^t}(\mathbf{x}^t | \mathbf{z}^{t-1}, \mathbf{a}^{t-1}; \boldsymbol{\theta}) \\ &= p_{Z^t}(\mathbf{z}^t | \mathbf{z}^{t-1}, \mathbf{a}^{t-1}; \boldsymbol{\theta}) \left| \frac{\partial \mathbf{z}^t}{\partial \mathbf{x}^t} \right| \\ &= \frac{p_{Z^t, Z^{t-1}}(\mathbf{z}^t, \mathbf{z}^{t-1} | \mathbf{a}^{t-1}, \boldsymbol{\theta})}{p_{Z^{t-1}}(\mathbf{z}^{t-1}; \boldsymbol{\theta})} \left| \frac{\partial \mathbf{z}^t}{\partial \mathbf{x}^t} \right| \end{aligned} \quad (4)$$

where $p_{X^t}(\mathbf{x}^t | \mathbf{x}^{t-1}, \mathbf{a}^{t-1}; \boldsymbol{\theta})$ and $p_{Z^t}(\mathbf{z}^t | \mathbf{z}^{t-1}, \mathbf{a}^{t-1}; \boldsymbol{\theta})$ are the distribution of \mathbf{x}^t conditional on \mathbf{x}^{t-1} and the distribution of \mathbf{z}^t conditional on \mathbf{z}^{t-1} , respectively. Then, the log-likelihood can be computed as follows:

$$\begin{aligned} \log p_{X^t}(\mathbf{x}^t | \mathbf{x}^{t-1}, \mathbf{a}^{t-1}; \boldsymbol{\theta}) &= \log p_{Z^t, Z^{t-1}}(\mathbf{z}^t, \mathbf{z}^{t-1} | \mathbf{a}^{t-1}, \boldsymbol{\theta}) \\ &\quad - \log p_{Z^{t-1}}(\mathbf{z}^{t-1}; \boldsymbol{\theta}) + \log \left| \frac{\partial \mathbf{z}^t}{\partial \mathbf{x}^t} \right| \end{aligned}$$

The Joint Distributions: In order to model the aging transformation flow, the Gaussian distribution is presented as the prior distribution p_Z for the latent space. After mapping to the latent space, the age controller variables are also constrained as a Gaussian distribution. In particular, let $\mathbf{z}_a^{t-1} = \mathbf{W}^a \mathbf{a}^{t-1}$ represent the latent variables of \mathbf{a}^{t-1} . The latent variables $\{\mathbf{z}^{t-1}, \bar{\mathbf{z}}^t, \mathbf{z}_a^{t-1}\}$ distribute as Gaussians with means $\{\boldsymbol{\mu}^{t-1}, \bar{\boldsymbol{\mu}}^t, \boldsymbol{\mu}_a^{t-1}\}$ and covariances $\{\Sigma^{t-1}, \bar{\Sigma}^t, \Sigma_a^{t-1}\}$ respectively. Then, the latent \mathbf{z}^t is as,

$$\begin{aligned} \mathbf{z}^t &\sim \mathcal{N}(\boldsymbol{\mu}^t, \Sigma^t) \\ \boldsymbol{\mu}^t &= \mathbf{W}(\mathbf{W}^z \boldsymbol{\mu}^{t-1} \odot \boldsymbol{\mu}_a^{t-1}) + \mathbf{b} + \bar{\boldsymbol{\mu}}^t \\ \Sigma^t &= \mathbf{W}[\mathbf{W}^z \Sigma^{t-1} \mathbf{W}^{z\top} \odot \Sigma_a^{t-1} \\ &\quad - (\mathbf{W}^z \boldsymbol{\mu}^{t-1})(\mathbf{W}^z \boldsymbol{\mu}^{t-1})^\top \odot \boldsymbol{\mu}_a^{t-1} \boldsymbol{\mu}_a^{t-1\top}] \mathbf{W}^\top \end{aligned} \quad (5)$$

Since the connection between \mathbf{z}^{t-1} and \mathbf{z}^t embeds the relationship between variables of different Gaussian distributions, we further assume that their joint distribution is also a Gaussian. Then, the joint distribution $p_{Z^t, Z^{t-1}}(\mathbf{z}^t, \mathbf{z}^{t-1} | \mathbf{a}^{t-1}; \boldsymbol{\theta})$ can be computed as follows.

$$\begin{aligned} p_{Z^t, Z^{t-1}}(\mathbf{z}^t, \mathbf{z}^{t-1} | \mathbf{a}^{t-1}; \boldsymbol{\theta}) &\sim \mathcal{N} \left(\begin{bmatrix} \boldsymbol{\mu}^t \\ \boldsymbol{\mu}^{t-1} \end{bmatrix}, \begin{bmatrix} \Sigma^t & \Sigma^{t, t-1} \\ \Sigma^{t-1, t} & \Sigma^{t-1} \end{bmatrix} \right) \\ \Sigma^{t, t-1} &= \mathbf{W}(\mathbf{W}^z \Sigma^{t-1} \odot \boldsymbol{\mu}_a^{t-1} \mathbf{1}^\top) \\ \Sigma^{t-1, t} &= (\mathbf{1} \boldsymbol{\mu}_a^{t-1\top} \odot \Sigma^{t-1} \mathbf{W}^{z\top}) \mathbf{W}^\top \end{aligned}$$

where $\mathbf{1} \in \mathbb{R}^D$ is an all-ones vector.

The Objective Function: The parameter $\boldsymbol{\theta}$ of the model is optimized to maximize the log-likelihood as in Eqn. (6).

$$\begin{aligned} \boldsymbol{\theta}^* &= \arg \max_{\boldsymbol{\theta}} \log p_{X^t}(\mathbf{x}^t | \mathbf{x}^{t-1}, \mathbf{a}^{t-1}; \boldsymbol{\theta}) \\ \text{s.t. } \mathbf{z}_a^{t-1} &= \mathbf{W}^a \mathbf{a}^{t-1} \text{ distributes as a Gaussian} \end{aligned} \quad (6)$$

This constraint is then incorporated to the objective function

$$\boldsymbol{\theta}^* = \arg \max_{\boldsymbol{\theta}} \log p_{X^t}(\mathbf{x}^t | \mathbf{x}^{t-1}, \mathbf{a}^{t-1}; \boldsymbol{\theta}) + l(\boldsymbol{\mu}_a^{t-1}, \Sigma_a^{t-1}; \mathbf{a}^{t-1})$$

where $l(\boldsymbol{\mu}_a^{t-1}, \Sigma_a^{t-1}; \mathbf{a}^{t-1})$ is the log-likelihood function of \mathbf{a}^{t-1} given mean $\boldsymbol{\mu}_a^{t-1}$ and variance Σ_a^{t-1} .

3.2. IRL Learning from Aging Sequence

In this section, we further extend the capability of our model by defining an *Subject-Dependent Aging Policy Network* to provide a *planning aging path* for the aging controller. Consequently, the synthesized sequence, i.e. $\{\mathbf{x}^1, \dots, \mathbf{x}^T\}$, is guaranteed to be the best choice in the face aging development for a given subject.

Let $\zeta_i = \{\mathbf{x}_i^1, \mathbf{a}_i^1, \dots, \mathbf{x}_i^T\}$ be the observed age sequence of the i -th subject and $\zeta = \{\zeta_1, \zeta_2, \dots, \zeta_M\}$ be the set of all M aging sequences in the dataset. The probability of a sequence ζ_i can be defined as $P(\zeta_i) = \frac{1}{Z} \exp(-E_\Gamma(\zeta_i))$ where $E_\Gamma(\zeta_i)$ is an energy function parameterized by Γ , and $Z = \sum_{\bar{\zeta}} \exp(-E_\Gamma(\bar{\zeta}))$ is the partition function computed using all possible aging sequences $\bar{\zeta}$. Then, the goal is to

learn a model such that the log-likelihood $\mathcal{L}(\zeta; \Gamma)$ of the observed aging sequences is maximized as follows:

$$\Gamma^* = \arg \max_{\Gamma} \mathcal{L}(\zeta; \Gamma) = \frac{1}{M} \log \prod_{\zeta_i \in \zeta} P(\zeta_i) \quad (7)$$

In Eqn. (7), if $E_{\Gamma}(\zeta_i)$ is considered as a form of a reward function, then the problem is equivalent to learning a policy network from a Reinforcement Learning (RL) system given a set of demonstrations ζ .

The reward function is the key element for policy learning in RL. However, **pre-defining a reasonable reward function for face aging synthesis is impossible in practice**. Indeed, it is very hard to measure the goodness of the age-progressed images even the ground-truth faces of the subject at these ages are available. Therefore, rather than pre-define an add-hoc aging reward, the energy $E_{\Gamma}(\zeta_i)$ is represented as a neural network with parameters Γ and adopted as a non-linear cost function of an *Inverse Reinforcement Learning* problem.

In this IRL system, Γ can be directly learned from the set of observed aging sequences ζ . Fig. 2(B) illustrates the structure of the proposed IRL framework. Based on this structure, given a set of aging sequences as demonstrations, not only the cost function can be learned to maximize the log-likelihood of observed age sequence but also the policy, i.e. predicting aging path for each individual, is obtained with respect to the optimized cost.

Mathematically, the IRL based age progression procedure can be formulated as follows. Let $\mathcal{M}_{irl} \{\mathcal{S}, \mathcal{A}, \mathcal{T}, \zeta, E_{\Gamma}\}$ be a Markov Decision Process (MDP) where $\{\mathcal{S}, \mathcal{A}, \mathcal{T}\}$ denote the state space, the action space, and the transition model, respectively. ζ is the set of observed aging sequences and E_{Γ} represents the cost function. Given an MDP \mathcal{M}_{irl} , our goal is to discover the unknown cost function E_{Γ} from the observation ζ as well as simultaneously extract the policy $q(\mathbf{a}^{t-1} | \mathbf{x}^{t-1})$ that minimizes the learned cost function.

State: The state $\mathbf{s}^t = [\mathbf{x}^t, age]$ is defined as a composition of two information, i.e. the face image \mathbf{x}^t at the t -th stage; and the age label of \mathbf{x}^t .

Action: Similar to the age controller, an action \mathbf{a}^t is defined as the amount of aging variations that the progression process should perform on state \mathbf{s}^t . Given \mathbf{s}^t , an action \mathbf{a}^t is selected by stochastically sampling from the action probability distribution. During testing, given the current state, the action with the highest probability is chosen for synthesizing process. Due to data availability where the largest aging distance between the starting and ending images of a sequence is 15, we choose the length of $N_a = 16$ (i.e. plus one state of \mathbf{a}^t where \mathbf{s}^t and \mathbf{s}^{t+1} has the same age).

Cost Function: The cost function plays a crucial role to guide the whole system to learn the sequential policies to obtain a specific aging path for each subject. Getting a state

Algorithm 1 Subject-Dependent Aging Policy Learning

Input: Observed M age sequence $\zeta = \{\zeta_1, \dots, \zeta_M\}$ where $\zeta_i = \{\mathbf{s}_i^1, \mathbf{a}_i^1, \dots, \mathbf{s}_i^T\}$.
Output: optimized cost params Γ and distribution $q(\zeta)$

- 1: **Initialization:** Randomly initialize policy distribution $q_{\Gamma}^1(\zeta)$ with a uniform distribution.
- 2: **for** $k = 1$ to K_1 **do**
- 3: Sample M aging paths from $q_{\Gamma}^k(\zeta)$.
- 4: **for** $i = 1$ to M **do**
- 5: Apply synthesis component in Section 3.1 given the i -th sampled aging path and the starting state \mathbf{s}_i^1 to obtain the sampled sequence $\bar{\zeta}_i$.
- 6: Add $\bar{\zeta}_i$ to $\zeta_{q_{\Gamma}^k}$
- 7: **end for**
- 8: **for** $i = 1$ to K_2 **do**
- 9: Sample a batch of observed sequence $\hat{\zeta} \subset \zeta$
- 10: Sample a batch of sampling sequence $\hat{\zeta}_{q_{\Gamma}^k} \subset \zeta_{q_{\Gamma}^k}$
- 11: $\zeta_q \leftarrow \hat{\zeta} \cup \hat{\zeta}_{q_{\Gamma}^k}$
- 12: Compute the gradient $\frac{d\mathcal{L}(\Gamma)}{d\Gamma}$ using Eqn. (9)
- 13: Update Γ using $\frac{d\mathcal{L}(\Gamma)}{d\Gamma}$
- 14: **end for**
- 15: Update $q_{\Gamma}^k(\zeta)$ with $\zeta_{q_{\Gamma}^k}$ and E_{Γ} to $q_{\Gamma}^{k+1}(\zeta)$ using [11].
- 16: **end for**

\mathbf{s}^t and \mathbf{a}^t as inputs, the cost function maps them to a value $c_{\Gamma}(\mathbf{s}^t, \mathbf{a}^t)$. Thus, the cost for the i -th aging sequence can be obtained as $E_{\Gamma}(\zeta_i) = \sum_t c_{\Gamma}(\mathbf{s}_i^t, \mathbf{a}_i^t)$. In order to learn a complex and nonlinear cost formulation, each $c_{\Gamma}(\mathbf{s}^t, \mathbf{a}^t)$ is approximated by a neural network with two hidden layers of 32 hidden units followed by Rectified Linear Unit (ReLU).

Policy: Given the cost function $c_{\Gamma}(\mathbf{s}_i^t, \mathbf{a}_i^t)$, the policy is presented as a Gaussian trajectory distribution $q(\zeta_i) = q(\mathbf{s}_i^1) \prod_t q(\mathbf{s}_i^{t+1} | \mathbf{s}_i^t, \mathbf{a}_i^t) q(\mathbf{a}_i^t | \mathbf{s}_i^t)$ and optimized respecting to the expected cost function $\mathbb{E}_{q(\zeta_i)}[E_{\Gamma}(\zeta_i)]$.

Given the defined state \mathbf{s}^t and action \mathbf{a}^t , the observation aging sequence ζ_i is redefined as $\zeta_i = \{\mathbf{s}_i^1, \mathbf{a}_i^1, \dots, \mathbf{s}_i^T\}$. The log-likelihood $\mathcal{L}(\zeta; \Gamma)$ in Eqn. (7) can be rewritten as,

$$\mathcal{L}(\zeta; \Gamma) = -\frac{1}{M} \sum_{\zeta_i \in \zeta} E_{\Gamma}(\zeta_i) - \log \sum_{\bar{\zeta}} \exp(-E_{\Gamma}(\bar{\zeta})) \quad (8)$$

Since the computation of the partition function is intractable, the sampling-based approach [6] is adopted to approximate the second term of $\mathcal{L}(\zeta; \Gamma)$ in Eqn. (8) by a set of aging sequences sampled from the distribution $q(\zeta)$.

$$\mathcal{L}(\zeta; \Gamma) \approx -\frac{1}{M} \sum_{\zeta_i \in \zeta} E_{\Gamma}(\zeta_i) - \log \frac{1}{N} \sum_{\zeta_j \in \zeta_q} \frac{\exp(-E_{\Gamma}(\zeta_j))}{q(\zeta_j)}$$

where N is the number of age sequences sampled from a sampling distribution q . Then the gradient is then given by

$$\nabla_{\Gamma} \mathcal{L} = -\frac{1}{M} \sum_{\zeta_i \in \zeta} \frac{dE_{\Gamma}(\zeta_i)}{d\Gamma} + \frac{1}{Z'} \sum_{\zeta_j \in \zeta_q} w_{\zeta_j} \frac{dE_{\Gamma}(\zeta_j)}{d\Gamma} \quad (9)$$

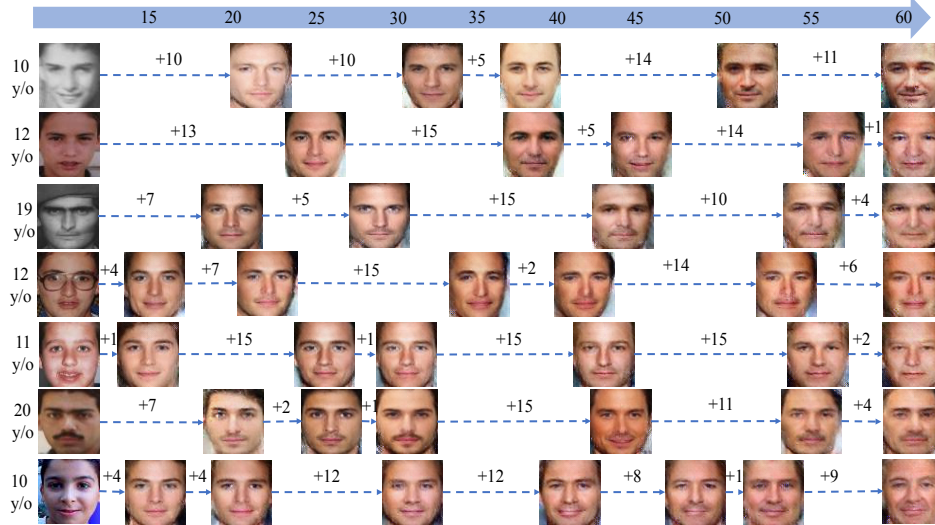


Figure 3: Age progression results on FG-NET. Given images at different ages and the target age of 60s, SDAP automatically predicts the optimal aging path and produce plausible age-progressed faces for each subject. **Best viewed in color.**

where $Z' = \sum_{\zeta_j} w_{\zeta_j}$ and $w_{\zeta_j} = \frac{\exp(-E_{\Gamma}(\zeta_j))}{q(\zeta_j)}$.

The choice of the distribution q is now critical to the success of the approximation. It can be adaptively optimized by first initialized with a uniform distribution and followed an iteratively three-step optimization process: (1) generate a set of aging sequences ζ_q ; (2) update the cost function using Eqn. (9); and (3) refine the distribution q as in Eqn. (10).

$$q^* = \arg \min_q \mathbb{E}_q [c_{\Gamma}(\zeta)] - \mathcal{H}(\zeta) \quad (10)$$

To solve Eqn. (10), we adopt the optimization approach [11] that also results in a policy $q(\mathbf{a}^t | \mathbf{s}^t)$. The Algorithm 1 presents the learning procedure in our policy network and cost function parameters.

Face aging with single and multiple inputs: During testing stage, given a face, its inputs, i.e. image and age, are used in the first state \mathbf{s}^1 . The action for \mathbf{s}^1 is predicted by the policy network. Then, the synthesis component can produce the age-progressed face for next state. This step is repeated until the age of the synthesized face reaches the target age.

Using this structure, the framework can be easily extended to take multiple inputs. Given n inputs to the framework, they are first ordered by ages and an input sequence $\{\mathbf{s}_0^1, \mathbf{a}_0^1, \dots, \mathbf{s}_0^n\}$ is created, where \mathbf{s}_0^i denotes the state with the i -th input face and age; and \mathbf{a}_0^i is the age difference between \mathbf{s}_0^i and \mathbf{s}_0^{i+1} . The synthesis component can be employed to obtain the values for latent variable \mathbf{z}_n^0 . This variable can act as “memory” that encodes all information from the inputs. We then initialize $\mathbf{s}^1 = [\mathcal{F}_2^{-1}(\mathbf{z}_n^0), \text{age}(\mathbf{s}_0^n)]$ and start the synthesis process as in the single input case.

4. Experimental Results

4.1. Databases

The proposed SDAP approach is trained and evaluated using two training and two testing databases that are not overlapped. The training sets consist of images from AgeInG Faces in the Wild [15] and aging sequences from Cross-Age Celebrity Dataset [4]. In testing, two common databases, i.e. FG-NET [1] and MORPH, [17] are employed.

AgeInG Faces in the Wild (AGFW): introduces a large-scale dataset with 18,685 images collected from search engines and mugshot images from public domains.

Cross-Age Celebrity Dataset (CACD) includes 163446 images of 2000 celebrities with the age range of 14 to 62.

FG-NET is a common testing database for both age estimation and synthesis. It includes 1002 images of 82 subjects with the age range is from 0 to 69 years old.

MORPH provides two albums with different scales. The small-scale album consists of 1690 images while the large-scale one includes 55134 images. We use the small-scale album in our evaluation.

4.2. Implementation Details

In order to train our SDAP model, we first extract the face regions of all images in AGFW and CACD and align them according to fix positions of two eyes and mouth corners. Then, we select all possible image pairs (at age t_1 and t_2) of a subset of 575 subjects from CACD such that $t_1 \leq t_2$ and obtain 13,667 training pairs. From the images of these subjects, we further construct the observed aging sequence set by ordering all images of each subject by age. This process produces 575 aging sequences. Using these training

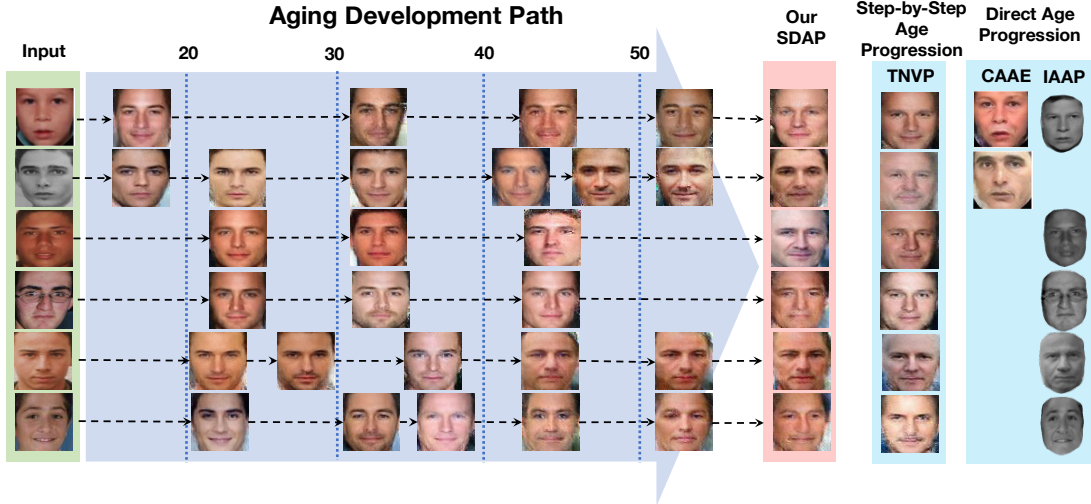


Figure 4: Comparisons between our SDAP against direct approach, i.e. IAAP [9], CAAE [26], and step-by-step approach, i.e. TNVP [14]. **Best viewed in color.**

data, we adopt the structure of mapping functions in [14] for our bijections $\mathcal{F}_1, \mathcal{F}_2$ and pretrain them using all images from AGFW for the capability of face interpretation. Then a two-step training process is applied. In the first step, the structure of synthesis unit with two functions $\mathcal{F}_1, \mathcal{F}_2$ and an age controller is employed to learn the aging transformation presented in all 13,667 training pairs. The synthesis units are then composed to formulate the synthesis component. Then in the second step, the Subject-Dependent Aging Policy Learning is applied to embed the aging relationships of observed face sequences and learn the Policy Network.

4.3. Age Progression

The structure of $\mathcal{F}_1, \mathcal{F}_2$ includes 10 mapping units where each unit is set up with 2 residual CNN blocks with 32 hidden feature maps for its scale and translation components. The convolution size is 3×3 . The training batch size is set to 64. A fully connected network with two layers is employed to build policy model. Each layer contains 32 units. The training time for our models is 24.75 hours in total on a machine with a Core i7-6700@3.4GHz CPU, 64.00 GB RAM and a GPU NVIDIA GTX Titan X. In reinforcement learning algorithm, *rllab* [5] framework is used to develop and evaluate our Algorithm 1.

Since our SDAP is trained using face sequences with age ranging from 10 to 64 years old, it is evaluated using all faces above ten years old in FG-NET and MORPH. Given faces of different subjects, our aging policy can find the optimal aging path to reach the target ages via intermediate age-progressed steps (Fig. 3). Indeed, SDAP not only produces aging path for each individual, but also well handles in-the-wild facial variations, e.g. poses, expressions, etc.

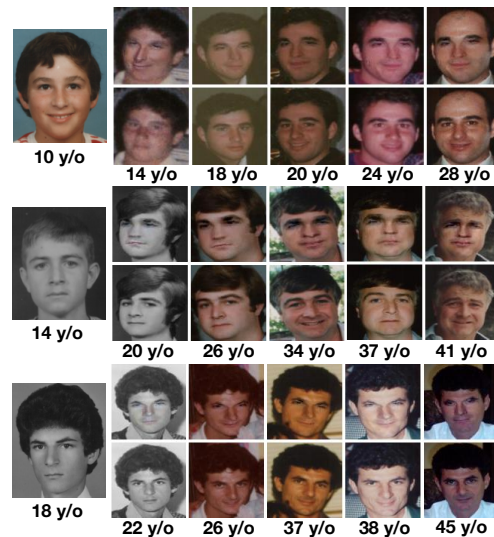


Figure 5: Age progression using SDAP. Given images (1st column), SDAP synthesizes the subject's faces at different ages (row above) against the ground-truth (row below).

In addition, the facial textures and shapes are also naturally and implicitly evolved according to individuals differences. In particular, more changes are focused around the ages of 20s, 40s and over 50s where beards and wrinkles naturally appear in the age-progressed faces around those ages. In Fig. 4, we further compare our synthesized results against other recent work, including IAAP [9], CAAE [26], and TNVP [14]. The predicted aging path of each subject is also displayed for reference. When the age distance between the input and target ages becomes large, the

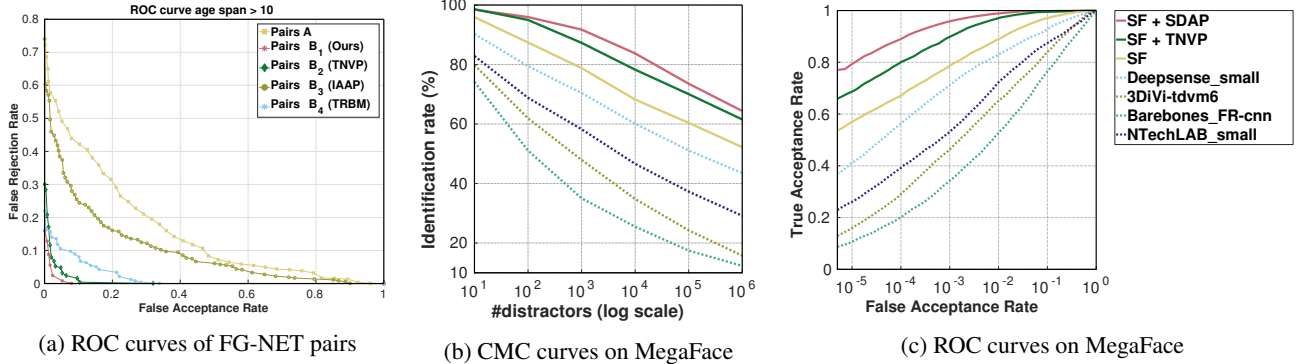


Figure 6: Comparison with other approaches in age invariant face recognition (a) ROC curves of face verification on the small-scale testing protocol; (b) Cumulative Match Curve (CMC) and (c) ROC curves of SF model [12] and its improvements using age-progressed faces from TNVP [14] and our SDAP on the large-scale testing protocol of MegaFace challenge 1.

direct age progression approaches usually produce synthesized faces that are similar to the input faces plus wrinkles. The step-by-step age progression tends to have better synthesis results but still limited in the amount of variations in synthesized faces. SDAP shows the advantages in the capability of capturing and producing more aging variations in faces of the same age group. Fig. 5 presents our further results at different ages with the real faces as reference.

4.4. Age Invariant Face Recognition

Our SDAP is also validated using the testing protocol as in [14] with two benchmarking sets of cross-age face verification. First, we perform *small-scale testing protocol* by constructing a set \mathbf{A} of 1052 randomly picked image pairs from FG-NET with age span larger than 10 years old. There are 526 positive pairs (the same subjects) and 526 negative pairs (different subjects). For each pair in \mathbf{A} , SDAP synthesizes the face of the younger age to the face of the older one. This process results in the set \mathbf{B}_1 . The same process is then applied using other age progression methods, i.e. IAAP [23], TRBM [15] and TNVP [14] to construct \mathbf{B}_2 , \mathbf{B}_3 and \mathbf{B}_4 , respectively. Then, the False Rejection Rate-False Acceptance Rate (FRR-FAR) is reported under the Receiver Operating Characteristic (ROC) curves as presented in Fig. 6a. These results show that our SDAP outperforms other age progression approaches with a significant improvement rate for matching performance over the original pairs.

In the *large-scale testing protocol*, we conduct Megaface [8] face verification benchmarking targeted on FG-NET plus one million distractors. Fig. 6b illustrates how the Rank-1 identification rates change when the number of distractors increases. The corresponding rates of all comparing methods at one million distractors are shown in Table 2. Fig. 6c presents the ROC curves respecting to True and False Acceptance Rates (TAR-FAR)¹. The Sphere Face

Table 2: Comparison results in Rank-1 Identification Accuracy with one million Distractors on MegaFace #1 FG-NET.

Methods	Training set	Accuracy
Barebones_FR	with cross-age faces	7.136 %
3DiVi	with cross-age faces	15.78 %
NTechLAB	with cross-age faces	29.168 %
DeepSense	with cross-age faces	43.54 %
SF [12]	without cross-age faces	52.22%
SF + TNVP [14]	without cross-age faces	61.53%
SF + SDAP	without cross-age faces	64.4%

(SF) model [12], trained solely on a small scale CASIA dataset having $< 0.49\text{M}$ images without cross-age information, achieves the best performance among all compared face matching approaches. Using our SDAP aging model, this face matching model can achieve even higher matching results in face verification. Moreover, these significant improvements gain without re-training the SF model and it outperforms other models as shown in Table 2.

5. Conclusions

This work has presented a novel Generative Probabilistic Modeling under an IRL approach to age progression. The model inherits the strengths of both probabilistic graphical model and recent advances of deep network. Given the tractable log-likelihood objective functions with deep features, high-quality age-progressed faces can be produced. In addition, our SDAP can provide a subject-dependent aging path with the optimal reward. It also allows multiple images as the inputs to enhance the optimal aging path for the subject. Finally, it requires simple preprocessing steps so that it can efficiently synthesize in-the-wild aging faces. The evaluations in quality of synthesized faces and cross-age verification show the robustness of the proposed

¹The results of other methods are provided in MegaFace website.

method.

References

- [1] *FG-NET Aging Database*. <http://www.fgnet.rsunit.com>.
- [2] G. Antipov, M. Baccouche, and J.-L. Dugelay. Face aging with conditional generative adversarial networks. *arXiv preprint arXiv:1702.01983*, 2017.
- [3] D. M. Burt and D. I. Perrett. Perception of age in adult caucasian male faces: Computer graphic manipulation of shape and colour information. *Proceedings of the Royal Society of London B: Biological Sciences*, 259(1355):137–143, 1995.
- [4] B.-C. Chen, C.-S. Chen, and W. H. Hsu. Cross-age reference coding for age-invariant face recognition and retrieval. In *ECCV*, 2014.
- [5] Y. Duan, X. Chen, R. Houthoofd, J. Schulman, and P. Abbeel. Benchmarking deep reinforcement learning for continuous control. In *International Conference on Machine Learning*, pages 1329–1338, 2016.
- [6] C. Finn, S. Levine, and P. Abbeel. Guided cost learning: Deep inverse optimal control via policy optimization. In *International Conference on Machine Learning*, pages 49–58, 2016.
- [7] X. Geng, Z.-H. Zhou, and K. Smith-Miles. Automatic age estimation based on facial aging patterns. *PAMI*, 29(12):2234–2240, 2007.
- [8] I. Kemelmacher-Shlizerman, S. M. Seitz, D. Miller, and E. Brossard. The megaface benchmark: 1 million faces for recognition at scale. In *CVPR*, 2016.
- [9] I. Kemelmacher-Shlizerman, S. Suwajanakorn, and S. M. Seitz. Illumination-aware age progression. In *CVPR*, pages 3334–3341. IEEE, 2014.
- [10] A. Lanitis, C. J. Taylor, and T. F. Cootes. Toward automatic simulation of aging effects on face images. *PAMI*, 24(4):442–455, 2002.
- [11] S. Levine and P. Abbeel. Learning neural network policies with guided policy search under unknown dynamics. In *Advances in Neural Information Processing Systems*, pages 1071–1079, 2014.
- [12] W. Liu, Y. Wen, Z. Yu, M. Li, B. Raj, and L. Song. Sphereface: Deep hypersphere embedding for face recognition. *arXiv preprint arXiv:1704.08063*, 2017.
- [13] K. Luu, C. Suen, T. Bui, and J. K. Ricanek. Automatic child-face age-progression based on heritability factors of familial faces. In *BldS*, pages 1–6. IEEE, 2009.
- [14] C. Nhan Duong, K. Gia Quach, K. Luu, N. Le, and M. Savvides. Temporal non-volume preserving approach to facial age-progression and age-invariant face recognition. In *The IEEE International Conference on Computer Vision (ICCV)*, Oct 2017.
- [15] C. Nhan Duong, K. Luu, K. Gia Quach, and T. D. Bui. Longitudinal face modeling via temporal deep restricted boltzmann machines. In *CVPR*, June 2016.
- [16] E. Patterson, K. Ricanek, M. Albert, and E. Boone. Automatic representation of adult aging in facial images. In *Proc. IASTED Intl Conf. Visualization, Imaging, and Image Processing*, pages 171–176, 2006.
- [17] K. Ricanek Jr and T. Tesafaye. Morph: A longitudinal image database of normal adult age-progression. In *FGR 2006*, pages 341–345. IEEE, 2006.
- [18] D. Rowland, D. Perrett, et al. Manipulating facial appearance through shape and color. *Computer Graphics and Applications, IEEE*, 15(5):70–76, 1995.
- [19] X. Shu, J. Tang, H. Lai, L. Liu, and S. Yan. Personalized age progression with aging dictionary. In *ICCV*, December 2015.
- [20] J. Suo, X. Chen, S. Shan, W. Gao, and Q. Dai. A concatenational graph evolution aging model. *PAMI*, 34(11):2083–2096, 2012.
- [21] J. Suo, S.-C. Zhu, S. Shan, and X. Chen. A compositional and dynamic model for face aging. *PAMI*, 32(3):385–401, 2010.
- [22] G. W. Taylor and G. E. Hinton. Factored conditional restricted boltzmann machines for modeling motion style. In *Proceedings of the 26th annual international conference on machine learning*, pages 1025–1032. ACM, 2009.
- [23] M.-H. Tsai, Y.-K. Liao, and I.-C. Lin. Human face aging with guided prediction and detail synthesis. *Multimedia tools and applications*, 72(1):801–824, 2014.
- [24] W. Wang, Z. Cui, Y. Yan, J. Feng, S. Yan, X. Shu, and N. Sebe. Recurrent face aging. In *CVPR*, pages 2378–2386, 2016.
- [25] H. Yang, D. Huang, Y. Wang, H. Wang, and Y. Tang. Face aging effect simulation using hidden factor analysis joint sparse representation. *TIP*, 25(6):2493–2507, 2016.
- [26] Z. Zhang, Y. Song, and H. Qi. Age progression/regression by conditional adversarial autoencoder. In *The IEEE Conference on Computer Vision and Pattern Recognition (CVPR)*, July 2017.